MULTI-SATELLITE MEASUREMENTS OF THE SUBSTORM INJECTION REGION

G. D. Reeves, T. A. Fritz, T. E. Cayton, R. D. Belian

Los Alamos National Laboratory, Los Alamos, NM

Abstract. Measurements of energetic particles obtained with a set of three geosynchronous satellites (1977-007, 1981-025, and 1982-019) are used to investigate the substorm injection region and particle drifts for an event on Feb. 3, 1983. A technique has been developed which allows remote sensing of the boundaries of the substorm injection region and the injection time by using measured energy dispersion and modeling particle drifts within the semi-empirical magnetospheric field model of Tsyganenko and Usmanov [1982]. The injection region for this event was found to span 90° around local midnight. The presence of spacecraft on either side of the injection region limit possible errors. Good agreement between long and short drift paths is found for ions while electron measurements give less reliable results.

Introduction

It has long been known that impulsive "injections" of plasma may be produced at geosynchronous orbit following substorms (eg. Arnoldy and Chan [1969], Belian et al. [1981]). In this paper we investigate the region of local time over which one substorm injection occurs. The data were obtained using Los Alamos Charged Particle Analyzer (CPA) instruments which have been flown on a series of satellites since 1976. A constellation of up to four geosynchronous satellites has been continuously maintained. The spin axis of each spacecraft is directed toward the Earth and protons are measured in the equatorial plane every 256 ms with two sets of detectors. The LoP detector monitors protons with 10 integral energy channels between ≈100 and ≈600 keV. (The integral energy channels are nested. Each has a different low energy threshold but shares a common high energy threshold.) The HiP detector measures protons with 16 differential energy channels from ≈0.4 to ≈150 MeV. Energetic electrons are also measured in the spacecraft equatorial plane by the HiE detector with six integral channels in the energy range ≈0.2 to ≈1.5 MeV. Electrons in the energy range ≈30 to ≈300 keV are measured in six energy channels by the LoE detector. The LoE instrument consists of a set of five integral detectors mounted at angles of 0°, ±30°, and

±60°. None of these spacecraft is equipped with a magnetometer. More complete descriptions of the CPA instruments can be found in Higbie et al. [1978], Belian et al. [1978], and Baker et al. [1979 and 1985].

This study uses the Tsyganenko and Usmanov [1982] magnetospheric field model which assumes analytic expressions for various current systems and fits parameters in those expressions to an extensive data set. It provides a model magnetic field vector at any point in the magnetosphere given the position, date, and time. The vector field is a superposition of the terrestrial field (IGRF 1982) and the Tsyganenko-Usmanov field (hereafter referred to as TU-82). We use this field to calculate the drift shells and trace the drifting particles.

Here we report an analysis of a single injection event and address the following questions: 1) Do the observations of this event support the standard model of injection of plasma near local midnight and subsequent gradient and curvature drift? 2) What is the range of local times over which energetic particles are injected? 3) How well do the simultaneous observations from the three satellites agree and what advantages do multi-point measurements provide? 4) How well does the TU-82 model reproduce the field configuration which was present during and after the injection?

Observations

The event we consider here occurred on Feb. 3, 1983 at ≈22.5 UT as evidenced by a negative bay observed in the magnetogram from Kiruna Sweden. The event was chosen primarily because it occurred during a fairly quiet time. Figure 1 shows the one minute average particle counts in three energy bands for electrons (a) and ions (b) on each of the three satellites. Plotted are differential count rates obtained by subtracting the count rates in two integral energy bands. A weak event producing mainly low energy electrons occurs near 19.0 UT. This event has little or no effect on the much stronger injection at 22.5 UT. The K_p indices in the 12 hours on either side of the event are all 2. The locations, in local time, of the three satellites at 22.5 UT is shown in Figure 2.

We consider the observations in terms of the "standard model" of substorm injections (see Pfitzer and Winckler [1969], Baker et al. [1979].) This model assumes that the injection occurs in a limited spatial region around local midnight, that the injection is impulsive, and that ions and electrons of all energies appear simultaneously. In a narrow band of energies such an injection appears as a pulse of

particles with a distinct onset, an abrupt rise in count rates, a peak and a decline. Under quiescent conditions, as for this event, an injection can produce easily recognized drift echoes which result from multiple drifts of particles around the Earth as a coherent population. Gradient-curvature drift produces eastward motion of electrons and westward motion of ions. As the pulse drifts it disperses. Dispersion in energy is seen both from one energy band to another and within a single energy band.

Simultaneous data taken at three local times provides a beautiful illustration of the drift of injected ion and electron pulses. Figure 1*a* shows that the onsets of enhanced electron fluxes for different energies measured at 1977-007 are simultaneous (they occur in the same 10 s spin-averaged bin) and that the rise from onset to peak is rapid (less than 10 min for the slowest electrons). The dispersionless signature observed at 1977-007 indicates that the satellite was within or very near the injection region. The 1981-025 satellite observes electrons which have drifted nearly half way around the Earth. The pulses arrive later and the arrival times show energy dispersion. The 1981-025 data also show that the leading edge of a pulse becomes less steep because of dispersion within a band. The electron pulses observed by 1982-019 show the same effects but to a greater degree. The next time the pulse for a particular energy band is observed is again at 1977-007 where it appears as a drift echo. The ions (Figure 1*b*) have a similar behavior. The time scales are shorter and the drifts are in the opposite sense with the ion pulses being observed by 1982-019, 1981-025, 1977-007, and again as a drift echo by 1982-019. (For drift echo studies see Lanzerotti et al. [1971], Brewer et al. [1969], Belian et al. [1978, 1981, and 1984]).

Analysis

The particle signatures show that 1977-007 was at a fortuitous position for this event. The electron signatures are dispersionless signifying local injection while the ion signatures for this satellite show dispersion. This indicates drift through a substantial distance. Assuming that the ions and electrons are injected quasi-neutrally these results imply that 1977-007 was located at the eastern-most edge of the injection region. The 1982-019 satellite was located near dusk The ions with energies of 195 keV arrive 6 min after the 320-keV ions indicating that 1982-019 lay outside the injection region. Thus these two satellites place limits on the injection region.

Using a model magnetic field we can extend the analysis to probe the boundaries of the injection region remotely using particle drifts. Typically drift analysis has been done using expressions which are valid in a dipole field (such as constant drift velocity). Here we use the TU-82 field model to determine the drift shells and to trace the drifting particles. To do so the field line connected to the satellite at the point of observation is traced and the first and second adiabatic invariants are determined. (Typically a pitch angle of 45° is used). A drift shell is calculated by searching for a set of discrete field lines on which the adiabatic invariants are conserved. The angular distance between two shell field lines is □□. The angular drift velocity at each shell field line is then calculated by numerically integrating the analytic expression for the bounce average drift velocity along the model field line. The time it takes particles of a given energy to drift through the angle □□ is □T. From the observation point at the satellite the calculation steps backward in time along the drift shell through 360°.

This analysis is repeated for each energy channel. The technique for determining the injection time and boundary is illustrated in Figure 3. The time that the arrival of an ion pulse was observed at 1982-019 is plotted against the location of the satellite and is shown in the figure by a dot. One line is plotted for each of the energy channels. Ideally the lines for different energies should meet at a single point which then gives the injection time and the location of the injection boundary. For the 1982-019 ion measurements they meet in a region centered on 22.48□UT and -42° from local midnight. Note that the time of injection determined from projecting the ion observations along the drift shell agrees well with the injection time which was observed directly in the electron data and in the Kiruna magnetogram.

We have repeated the analysis for the 1977-007 and 1981-025 ion measurements and for electron measurements from 1981-025 and 1982-019. The results are shown in Figure 4. The location of the satellites at 22.5□UT is plotted with circles, the westward injection boundaries calculated from ion data are plotted with triangles, and the eastward boundaries calculated from electron data are plotted with squares. The shading indicates which satellite the point is associated with (eg. gray for 1982-019). The drift shells are represented by the projection of the magnetic equator into the ecliptic plane (the GSE X-Y plane).

Figure 4 shows that the ion projections agree quite well (to within 10°) while the electron projections show significant disagreement. The agreement of the ion projections, even

though two must subtend large angles, give us confidence that the TU-82 model is a reasonable representation of the global field following the injection. There are several possible causes of the discrepancy in the electron projections. Firstly, we note that the electron measurements span a lower energy range and hence drift more slowly allowing more time for changes in the magnetic field or dispersive effects. The electrons are also more strongly affected by electric fields which are present but which have not been included in our drift calculation. We also notice that the the electron projections indicate that the model drifts are consistently too slow. This may be due to the wrong choice of pitch angles. The 45° pitch angle which was used gives good agreement between the measured and model ion drift periods but 90° may be more appropriate for electrons.

As a final note we return to the particle data to see if it is consistent with a 90° injection region. The top plot in Figure 5 shows ions measured at 1982-019 and the bottom plot shows electrons measured at 1977-007. The shaded area is the length of time it would take particles with the lowest energy in the band to drift through the entire 90° injection region beginning at the observed pulse onset. We find that for all energies the duration of the pulse is longer than the 90° drift time. Further, as we go to higher energies, the pulse duration and the 90° drift time become nearly equal. The data, therefore, are consistent with the 90° injection region but also indicate that the injection was not instantaneous.

Conclusions

We have analyzed the substorm injection event of Feb. 3, 1983 and found that it supports the standard model of substorm injections. Our results support the idea that energetic particles are injected in a range of local times around midnight and that ions and electrons of all energies are injected simultaneously. The time of arrival as measured directly and determined remotely through energy dispersion and particle tracing agree to within a few minutes at 22.5 UT. The observed motion of the resulting electron and ion pulses show the effects of gradient and curvature drifts and the presence of regularly periodic drift echoes implies that the magnetic configuration of the drift shells as a whole change little in the hours following the injection. The injection was determined to span 90° in local time and that extent was found to be consistent with the duration of the pulses. The availability of multi-satellite measurements greatly enhances the reliability of the remote sensing. The presence of a satellite located near both the eastward and westward

boundaries of the injection region reduces the dependence of the results on the details of the magnetic field model and mitigates errors which could be introduced if only single satellite measurements were used. This capability also facilitates distinguishing spatial from temporal effects. Finally, although the TU-82 model is limited in its ability to accurately represent the real field we feel that a semi-empirical field model which includes a good internal field and realistic noon-midnight asymmetries is essential for using remote observations to probe substorm injection processes.

Acknowledgements. The authors would like to thank David Stern and Harlan Spence for the use of their TU-82 model code and S. Peter Gary for critical reading of the manuscript.

References

Arnoldy, R. L., and K. W. Chan, Particle substorms observed at geostationary orbit, *J. Geophys. Res., 7*, 5019, 1969.

Baker, D. N., R. D. Belian, P. R. Higbie, and E. W. Hones, High-energy magnetospheric protons and their dependence on geomagnetic and interplanetary conditions, *J. Geophys. Res., 84*, 7138, 1979.

Baker, D. N., W. Aiello, J. R. Asbridge, R. D. Belian, P. R. Higbie, R. W. Klebesadel, J. G. Laros, and E. R. Tech, Los Alamos energetic particle sensor systems at geostationary orbit, *AIAA Proc., Reno Nevada*, January 14-17, 1985.

Belian, R. D., D. N. Baker, P. R. Higbie, and E. W. Hones, High-resolution energetic particle measurements at 6.6 Re 2: High-energy proton drift echoes, *J. Geophys. Res., 83*, 4857, 1978.

Belian, R. D., D. N. Baker, E. W. Hones, P. R. Higbie, S. J. Bame, and J. R. Asbridge, Timing of energetic proton enhancements relative to magnetospheric substorm activity and its implication for substorm theories, *J. Geophys. Res., 86*, 1415, 1981.

Belian, R. D., D. N. Baker, E. W. Hones, and P. R. Higbie, High-energy proton drift echoes: Multiple peak structure, *J. Geophys. Res., 89*, 9101, 1984.

Brewer, H. R., M. Schultz, and Aharon Eviatar, Origin of drift-periodic echoes in outer-zone electron flux, *J. Geophys. Res., 74*, 159, 1969.

Higbie, P. R., R. D. Belian, and D. N. Baker, High-resolution energetic particle measurements at 6.6 Re 1: Electron micropulsations, *J. Geophys. Res., 83*, 4857, 1978.

Lanzerotti, L. J., C. G. Maclennan, and M. F. Robins, Proton drift echoes in the magnetosphere, *J. Geophys. Res., 76*, 259, 1971.

Pfitzer, K. A., and J. R. Winckler, Density correlations and substorm electron drift effects in the outer radiation belt measured with the OGO-3 and ATS-1 satellites, *J. Geophys. Res., 74*, 5005, 1969.

Tsyganenko, N. A., and A. V. Usmanov, Determination of the magnetospheric current system parameters and development of experimental geomagnetic field models based on data from IMP and HEOS satellites, *Planet. Space Sci., 30*, 985, 1982.

_____

R. D. Belian, T. E. Cayton, T. A. Fritz, and G. D. Reeves, Los Alamos National Laboratory, Los Alamos, NM

(submitted March 12, 1990;
revised June 8, 1990;
accepted August 1, 1990.)

Paper number 90L6418
0148-0227/88/88JA03596$03.00

Paper number 90L6418

Reeves et al: Measurements of the Substorm Injection Region

Reeves et al: Measurements of the Substorm Injection Region

Reeves et al: Measurements of the Substorm Injection Region

Fig. 1. One minute average differential count rates for electrons (A) and ions (B). Three differential energy curves are given for each of the three satellites. Particle drifts and dispersion are seen which are consistent with the standard substorm injection model. (See Figure 2 for the positions of the satellites.)

Fig. 2. The location of the three geosynchronous satellites and a schematic representation of the substorm injection and particle drifts are shown.

Fig. 3. The dots show the time and location of ion injection onsets measured in nine energy channels on 1982-019 for the Feb. 3, 1983 event. The solid lines represent projections of the injection onsets backward in time along the drift shell as described in the text. The intersection of the lines gives the injection boundary location and injection time.

Fig. 4. The injection region. Satellite locations (circles), projected ion injection boundaries (triangles), projected electron boundaries (squares), and equatorial drift shells are plotted in the GSE ecliptic plane. Points for 1977-007 are filled with white, 1981-025 with black, and 1982-019 with gray. The injection region is determined to span 90° in local time around midnight.

Fig. 5. One minute average particle count rates for ions measured by 1982-019 and electrons measured by 1977-007. The shaded area shows the time it takes for particles to drift through the 90° injection region. Ion and electron echoes are also apparent.

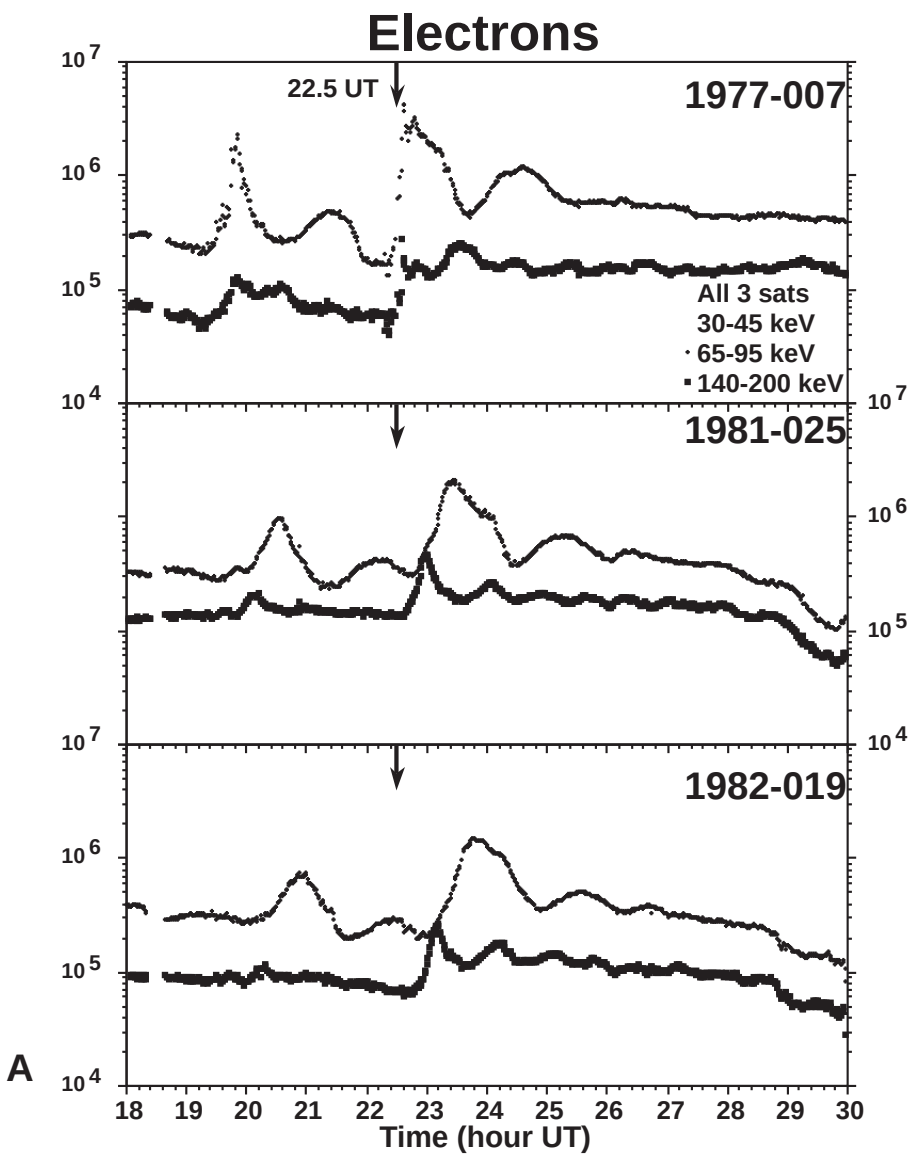
Electrons
22.5 UT
1977-007
All 3 sats
30-45 keV
65-95 keV
140-200 keV
1981-025
1982-019
A
Time (hour UT)

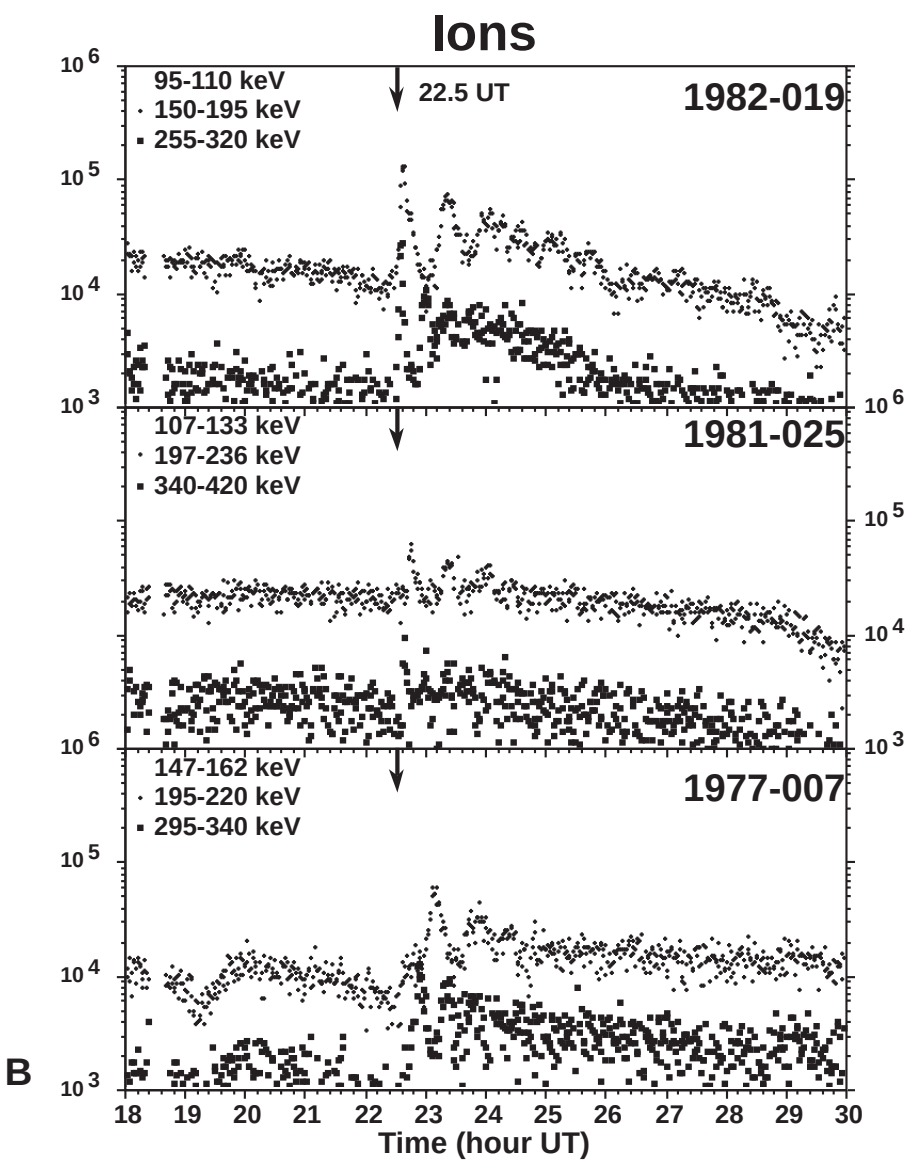
Ions
95-110 keV
150-195 keV
255-320 keV
22.5 UT
1982-019
107-133 keV
197-236 keV
340-420 keV
1981-025
147-162 keV
195-220 keV
295-340 keV
1977-007
B
Time (hour UT)

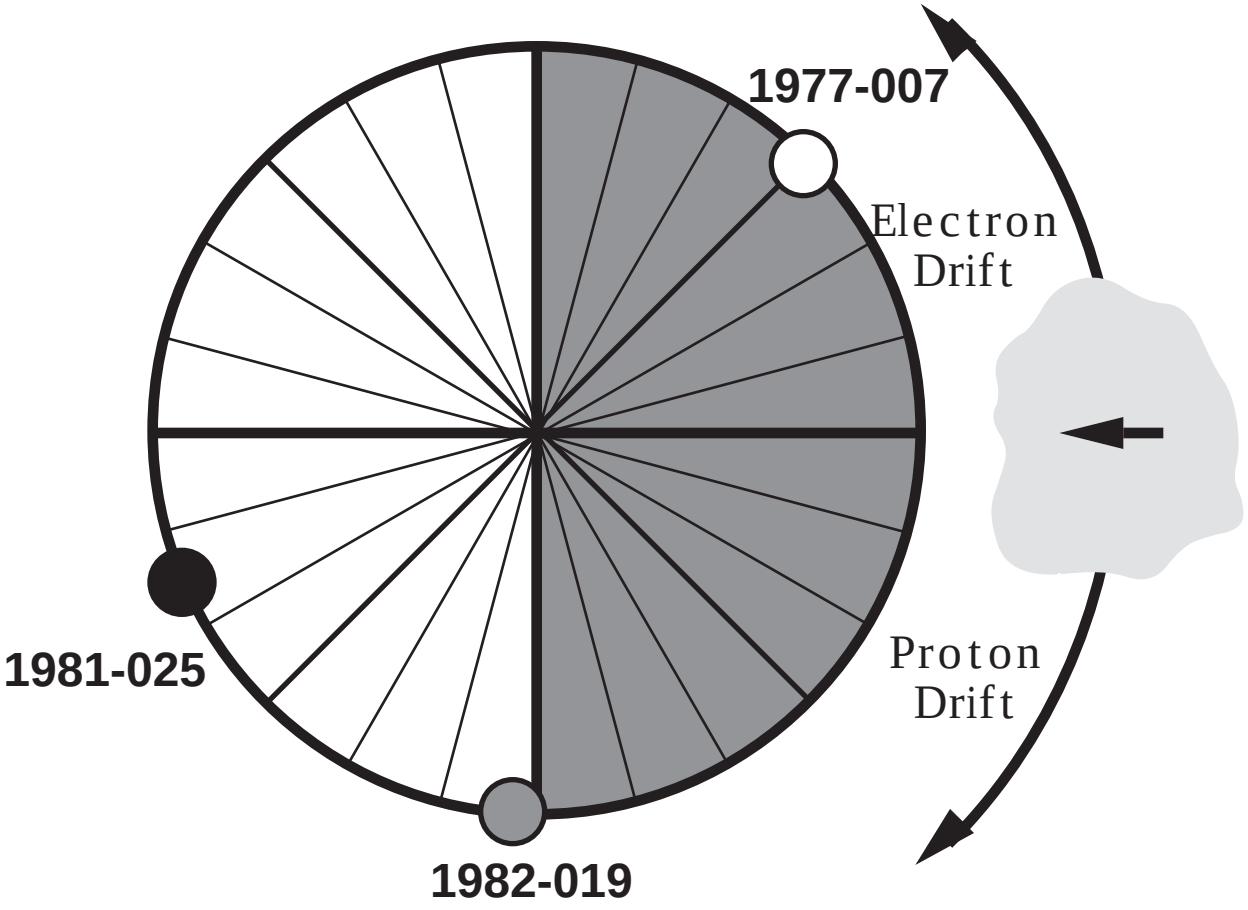
1977-007
Electron
Drift
1981-025
Proton
Drift
1982-019

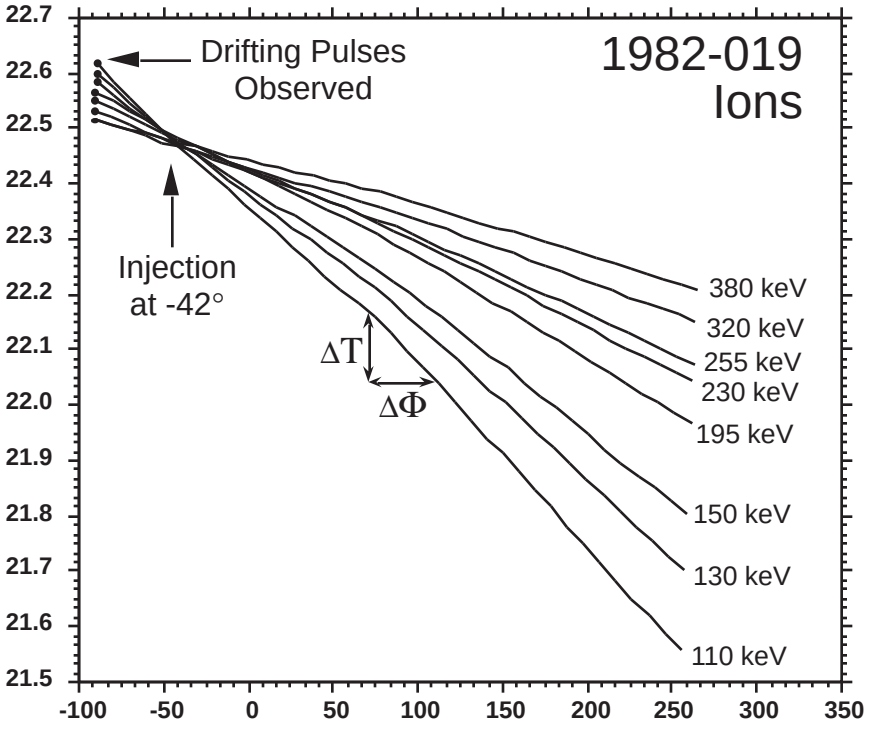
1982-019
Ions
Drifting Pulses
Observed
Injection
at -42°
ΔT
ΔΦ
380 keV
320 keV
255 keV
230 keV
195 keV
150 keV
130 keV
110 keV
22.7
22.6
22.5
22.4
22.3
22.2
22.1
22.0
21.9
21.8
21.7
21.6
21.5
-100
-50
0
50
100
150
200
250
300
350
Degrees from Local Midnight

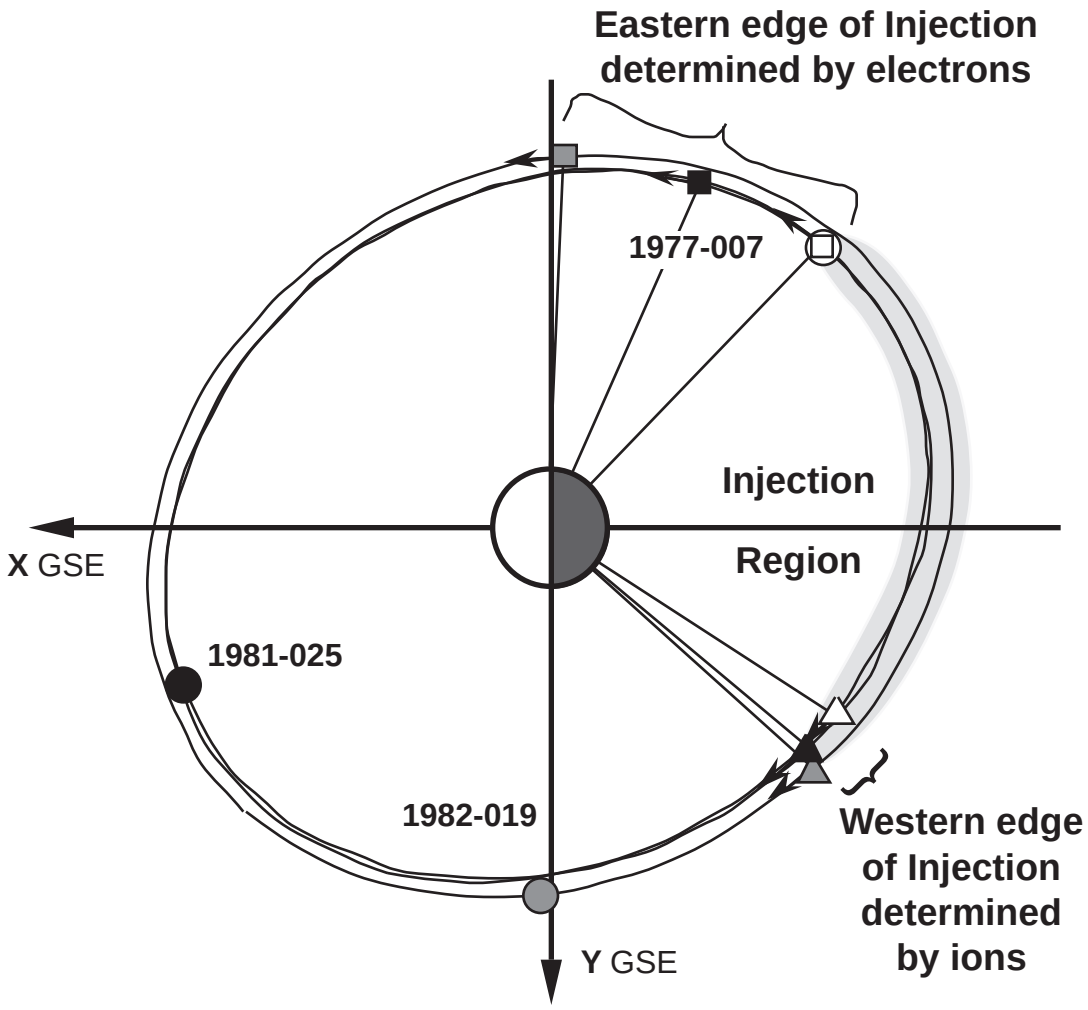
Eastern edge of Injection
determined by electrons
1977-007
Injection
Region
X GSE
1981-025
1982-019
Western edge
of Injection
determined
by ions
Y GSE

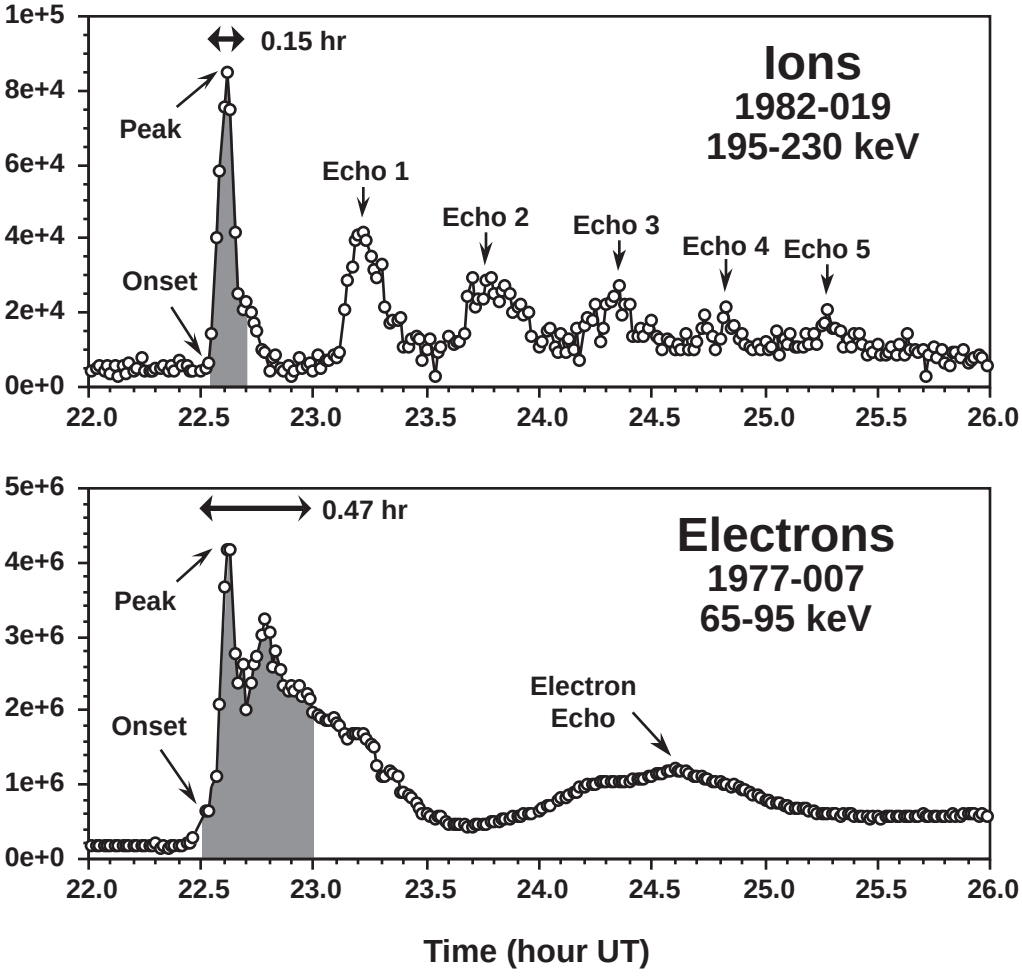
1e+5
8e+4
6e+4
4e+4
2e+4
0e+0
0.15 hr
Peak
Onset
Echo 1
Echo 2
Echo 3
Echo 4
Echo 5
Ions
1982-019
195-230 keV
22.0
22.5
23.0
23.5
24.0
24.5
25.0
25.5
26.0
5e+6
4e+6
3e+6
2e+6
1e+6
0e+0
0.47 hr
Peak
Onset
Electron
Echo
Electrons
1977-007
65-95 keV
Time (hour UT)